5.5. Ushuaia, Argentina

The Ushuaia installation is near the southern port city of Ushuaia, Argentina, at the Centro Austral de Investigaciones Cientificas (CADIC) facility. CADIC is a regional research center of the National Research Council of Argentina (CONICET). A Global Atmospheric Watch (GAW) is also located at Ushuaia. The installation is located in the foothills of the Andes and is subject to frequent clouds. The Ushuaia SUV-100 instrument is installed in the roof of the main CADIC building and is relatively free of obstructions.

The Ushuaia installation was the fourth site established in the network. Initially, many problems occurred resulting in a data set with frequent gaps. These problems resulted from difficulties in sending equipment to Ushuaia, temperature instability at the installation site, and frequent power failures. Since September 1990, however, the situation has improved, resulting in stable system operation. In December 1991, a UPS was installed and the power outage disruptions in data have been reduced. A further reduction in interruptions occurred after modifications were conducted during the March 1992 site visit. Minor system upgrades have been installed in subsequent years.

Because of the initial problems with the system, some of the data reported on CD-ROM Volume 1.0 were underestimated by approximately 8% (see Section 6). The corrected data (on the Volume 2 CD-ROM) are now available upon request from Biospherical Instruments Inc. Also, some minor gaps existed in the data. Many of these gaps have been restored and are now available.

The data are originally recorded onto both a 120-MB removable hard disk media and a hard disk drive internal to the system control computer. Archiving is automated. The system control computer, utilizing the Windows NT® operating system and direct dial-up (via modem) to a local Internet service provider, allows for direct data transmission (FTP'd to a BSI server), by the operator on-site. Files can also be transferred as e-mail attachments.

Figure 5.5.1. *Roof box portion of the spectroradiometer installed in the roof of the CADIC facility in Ushuaia.*

Table 5.5.1. Obstructions in the collector's field-of-view at Ushuaia.

Feature	Range (degrees)	Elevation (degrees)
mountains	8° - 33°	6.5°
mountains, buildings	33° - 120°	4°
mountains, across channel	120° - 206°	2.5°
distant mountains	206° - 240°	4°
Mt. Susana	240° - 253°	4°
distant mountains	253° - 286°	4°
mountains	286° - 298°	10°
CADIC water tower	298° - 302°	17°
mountains	302° - 8°	10°

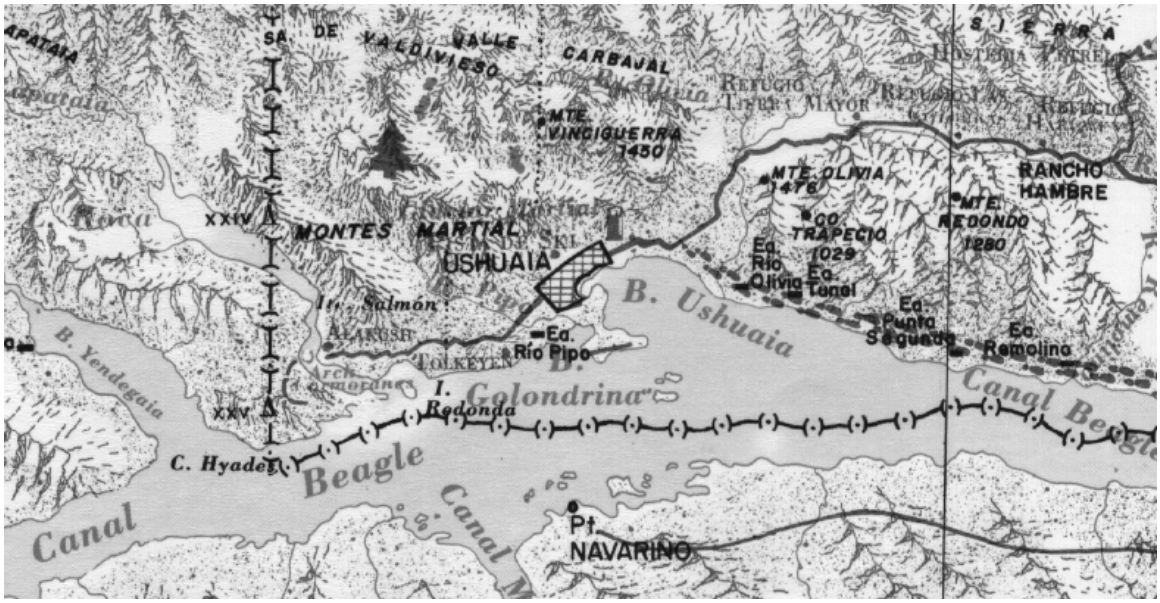

Figure 5.5.2. *Map of Ushuaia and vicinity.*

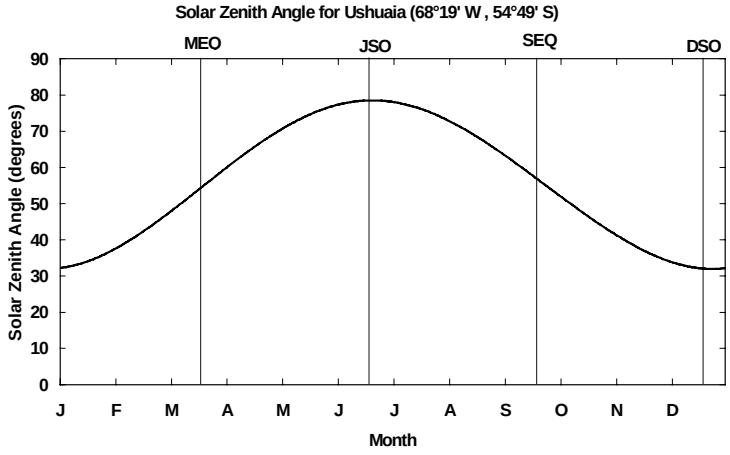

Figure 5.5.3. *Noontime solar zenith angle during the year at Ushuaia.*

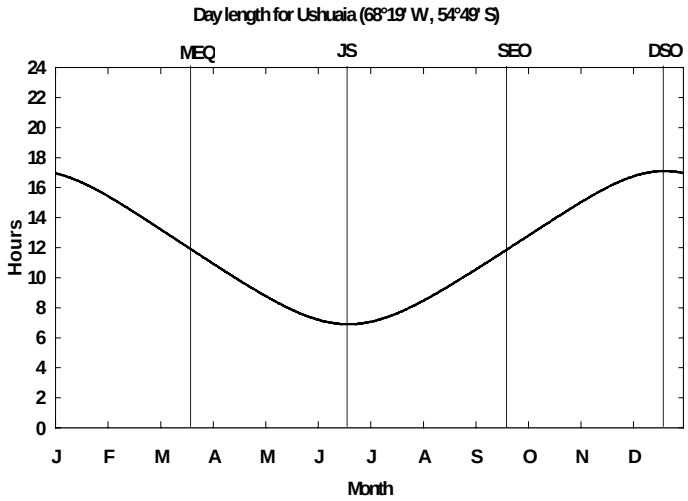

Figure 5.5.4. *Day length for Ushuaia. (MEQ = March equinox, JSO = June solstice, SEQ = September equinox, DSO = December solstice).*

5.5.1. Weather Observations

Weather observations for Ushuaia (WMO station number 87938) were obtained from the National Climatic Data Center (NCDC). The data are in a format described in Appendix A7 of this report. The file, USHUAIA.CSV, can be found in the \WEATHER directory on the CD-ROM 7.0.a.

5.5.2. Ozone Observations

Table 5.5.2. TOMS ozone averages and minima for Ushuaia, September 1 – December 31.

	TOMS												TOVS		
	Nimbus 7			Meteor 3			Adeos			Earth Probe					
Year	Avg	Min	Date	Avg	Min	Date	Avg	Min	Date	Avg	Min	Date	Avg	Min	Date
1988	329.0	231	10/21/88												
1989	327.7	217	10/16/89												
1990	312.4	200	10/13/90												
1991	315.1	189	10/23/91	313.1	185	10/8/91									
1992	314.6	155	10/5/92	312.5	162	10/6/92									
1993				302.7	190	9/27/93									
1994				293.9	158	10/17/94							303.5	172	10/17/94
1995													308.9	220	10/14/95
1996							319.1	215	11/23/96	321.5	196	9/17/96	313.9	201	9/17/96
1997										309.4	190	10/14/97			
1998										315.4	177	9/30/98			

Note: 1996 TOMS/Adeos data is only partially available; actual data starts on 9/11/96. 1998 TOMS/Earth Probe data is not available after 12/12/98. The average was therefore calculated from the period 9/1/98 – 12/12/98.

Records from TOMS/Earth Probe indicate that minima in ozone decreased between 1996 and 1998. The minimum value in the Volume 7 Ushuaia season was 190 DU on 10/14/97.

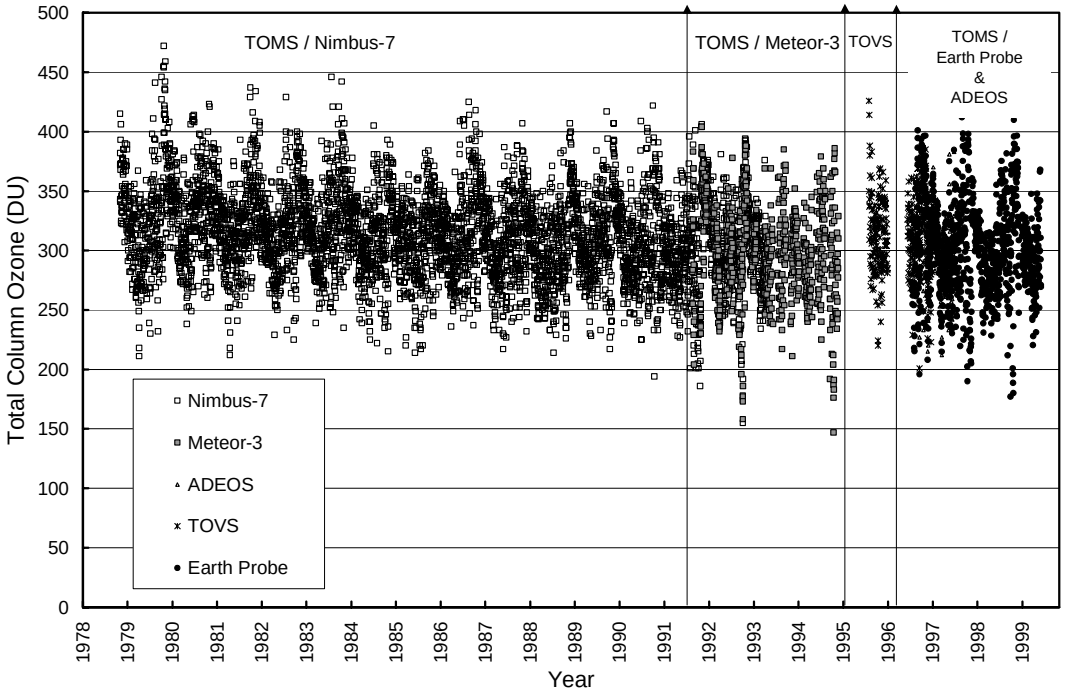

Figure 5.5.5. *Time record of total column ozone from TOMS and TOVS data at Ushuaia.*

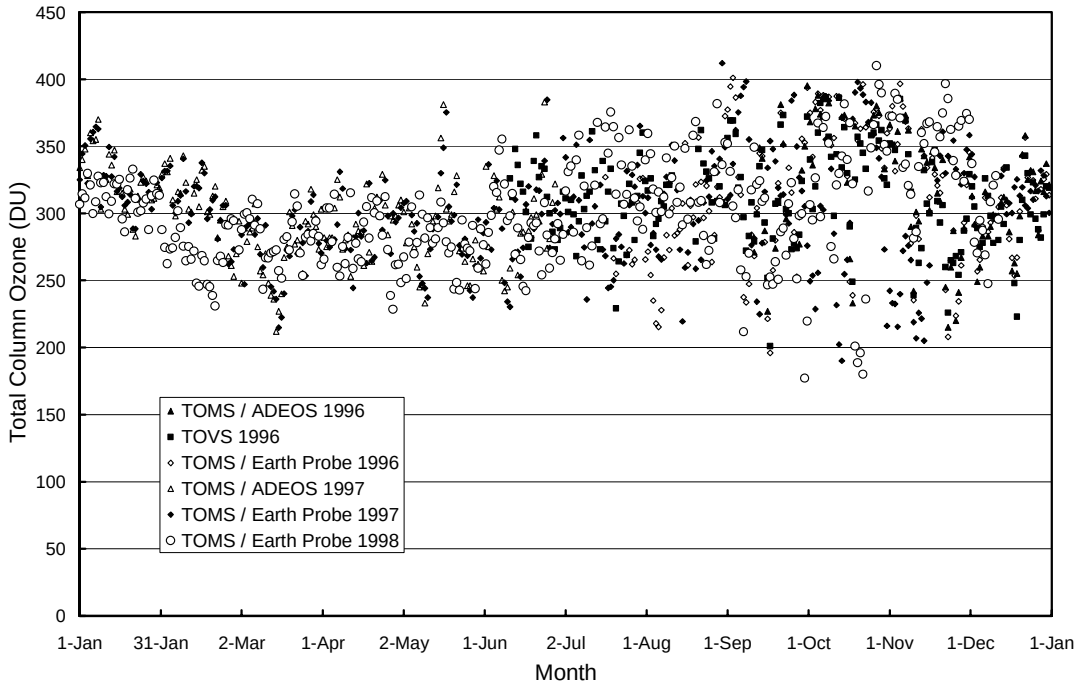

Figure 5.5.6. *Seasonal variation in ozone from TOMS and TOVS data at Ushuaia. The variability later in the year is much higher than earlier in the year.*

5.5.3. Ushuaia 3/25/97-4/19/98

The 1997/98 season at Ushuaia is defined as the time between the site visits, 3/25/97 – 4/1/97 and 4/11/98 – 4/19/98. The season opening and closing calibrations were performed on 3/30/97 and 4/11/98, respectively. Solar data is available for the period 4/2/97 – 4/10/98. During this time the system operated normally. In the first months of the season, however, the sensitivity of the instrument was set too high leading to saturation in several data and response lamp scans. Affected data were excluded from the volume. In the middle of the season, measurements of the response lamp were unstable. This was most likely caused by wobbly contact of the response lamp's terminals. For these days, the responsivity of the instrument could not be derived from the daily response scans but was taken from scans preceding or succeeding the affected day. The good scans taken during this period showed that the instrument itself was quite stable. Therefore the accuracy of solar data was only slightly affected.

5.5.3.1. Stability in the Wavelength Domain

As for the other sites, wavelength stability of the system was monitored with the internal Mercury lamp. Information from the daily wavelength scans was used to homogenize the data set by correcting day-to-day fluctuations of the wavelength offset. After this step, there may still be a deviation from the correct wavelength scale but this bias should ideally be the same for all days. Figure 5.5.7 shows the differences in the wavelength offset of the 296.73 nm Mercury line between two consecutive wavelength scans. In total, 374 scans have been evaluated. For 76% of the days, the change in offset is smaller than ±0.025 nm; for 91% of the days the shift is smaller than ±0.055 nm. For 4% of the scans the offset-difference is larger than ±0.1 nm. Compared to other sites, this is a relatively large number and is caused by frequent power outages. The capacity of the uninteruptable power supply (UPS) installed at Ushuaia was often not sufficient and was therefore upgraded in the following season. After a power cut the wavelength position had to be adjusted manually and the new wavelength position was determined thereafter with a manual wavelength scan. Succeeding data scans were paired with this wavelength scan and the power outages therefore did not affect the wavelength accuracy of the solar data.

After the data was corrected for day-to-day wavelength fluctuations, the wavelength-dependent bias between this homogenized data set and the correct wavelength scale was determined with the Fraunhofer-correlation method, as described in Section 3. The thick line in Figure 5.5.8 shows the resulting correction function that was applied to the Volume 7 Ushuaia data. The wavelength-dependence of the function is caused by the non-linearities of the monochromator drive. In order to demonstrate the difference between the result of the new Fraunhofer-correlation method and the method that was historically applied, Figure 5.5.8 also includes a correction function that was calculated with the old method, i.e., the function is based on internal wavelength scans only. The average difference between both approaches is 0.083 nm. As explained in Section 3, the different light paths for internal wavelength scans and solar measurements cause this bias.

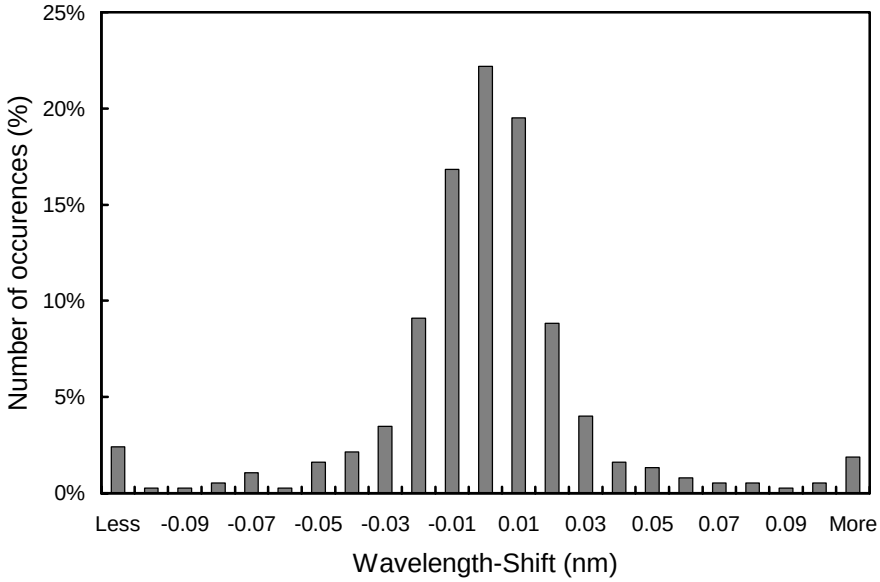

Figure 5.5.7. *Differences in the measured position of the 296.73 nm Mercury line between consecutive wavelength scans. The x-labels give the center wavelength shift for each column. Thus the 0-nm histogram column covers the range -0.005 to +0.005 nm. "Less" means shifts smaller than –0.105 nm; "more" means shifts larger than 0.105 nm.*

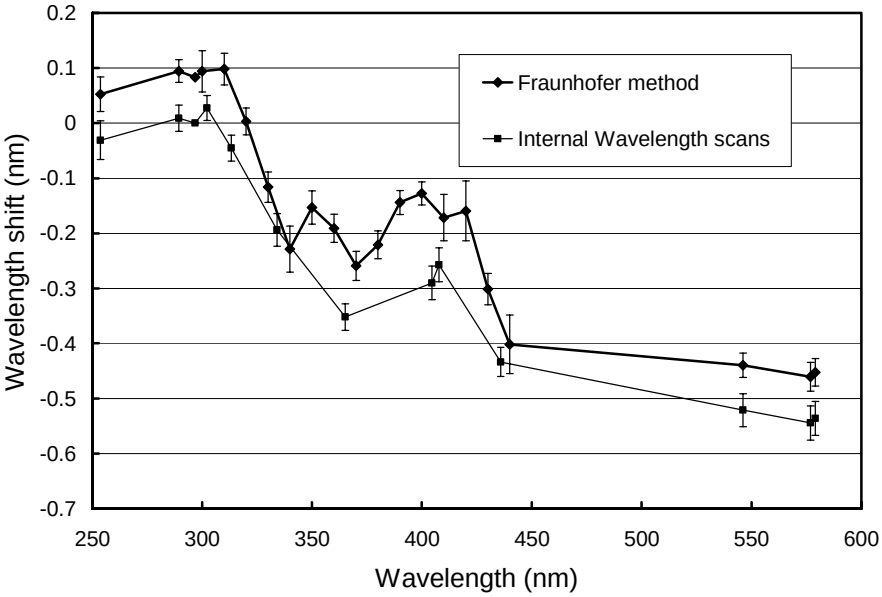

Figure 5.5.8. *Functions expressing the monochromator non-linearity for Ushuaia. Thick line: Function calculated with the Fraunhofer-correlation method. This function was applied to correct the Ushuaia Volume 7 data. Thin line: Function calculated with the method that was historically applied. The offset between the two methods is 0.083 nm. Both functions represent average wavelength shifts for the 1997/98 season. The error bars give the 1σ standard deviation variation of the wavelength shifts.*

After the data was wavelength corrected using the shift-function described above, the wavelength accuracy was tested again with the Fraunhofer method. The result is shown in Figure 5.5.9. At 320 nm, the wavelength shift for noontime measurements is smaller than ±0.075 nm throughout the season; most shifts

are in a ±0.05 nm range. The actual wavelength uncertainty may be a little larger because of wavelength fluctuations of about ±0.02 nm during a day and possible systematic errors of the Fraunhofer correlation method (see Section 3). The shifts for other wavelengths in the UV have a very similar pattern to the shift at 320 nm presented in Figure 5.5.9.

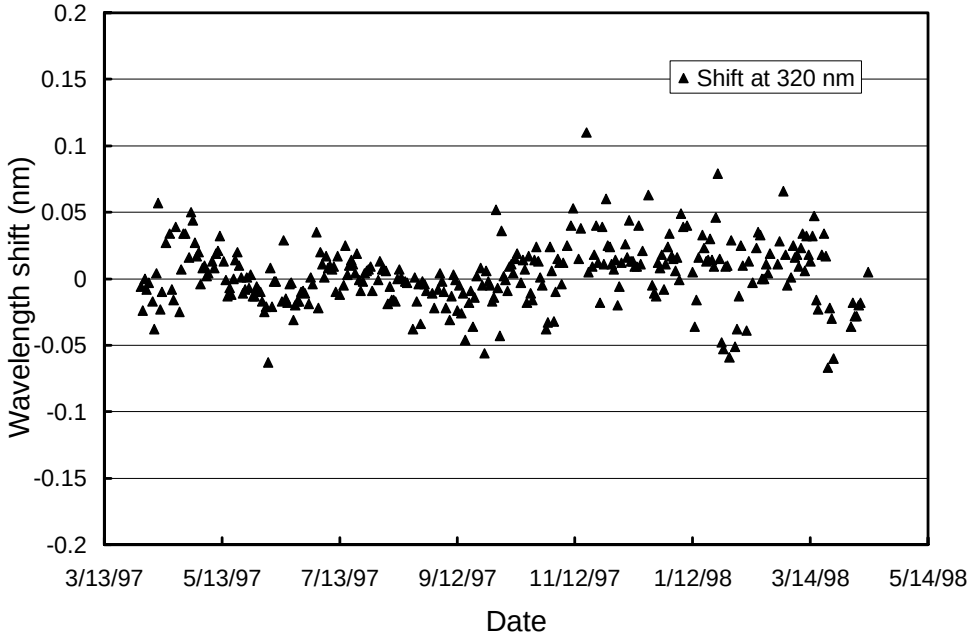

Figure 5.5.9. *Check of the wavelength accuracy of the final data by means of Fraunhofer correlation. For each day of the season the noontime measurement has been evaluated. The shift is smaller than ±0.05 nm for most days.*

Although the data from the external mercury scans do not have a direct influence on the data products, they are an important part of instrument characterization. Figure 5.5.10 illustrates the difference between internal and external Mercury scans collected during both site visits. External scans have a bandwidth of about 1.03 nm FWHM, whereas the bandwidth of the internal scan is only 0.72 nm. In addition, the peak of external scans is shifted towards longer wavelengths compared to the internal peak. Since external scans have the same light path as solar measurements, they more realistically represent the bandpass of the monochromator. The scans at the start and end of the season are very consistent, as can be seen from Figure 5.5.10.

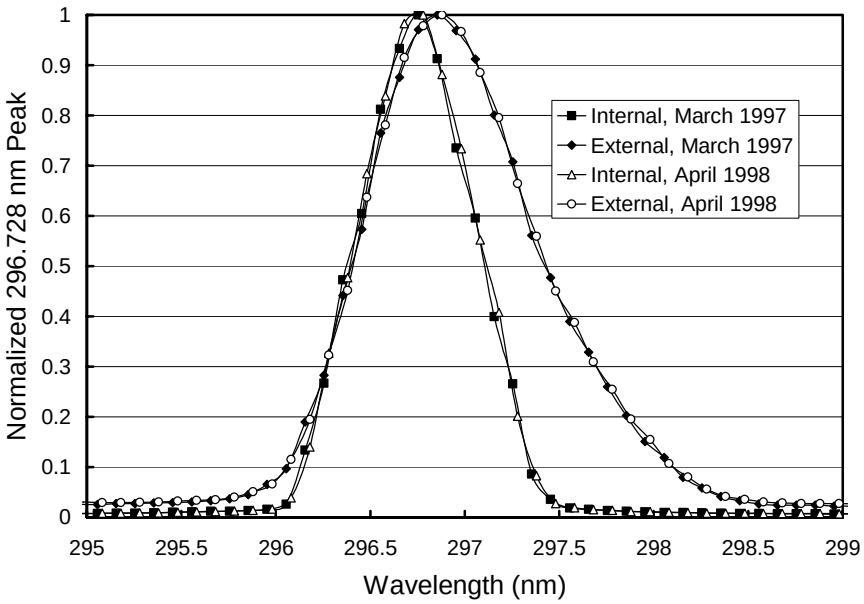

Figure 5.5.10. *The 296.73 mercury spectral line as registered by the PMT from external and internal source.*

5.5.3.2. Responsivity Stability

The stability of the spectroradiometer's responsivity over time is monitored with the internal response lamp. In the middle of the Volume 7 Ushuaia season, the contact between the response lamp's terminals and the lampholder became somewhat loose. This might have been caused by thermal stress during previous operation of the lamp and led to unstable response lamp measurements. For the affected days, the responsivity of the instrument could not be derived from the daily response scan but was taken from scans preceding or succeeding the affected day. The following figures show that the good scans indicate that the instrument itself was quite stable. Therefore the accuracy of solar data is only slightly affected. As a final proof of the instrument's stability solar spectral measurements were weighted with the responsivity function of the TSI and compared with the TSI signal. For a given solar zenith angle range, the ratio of both measurements is stable over the whole period to within ±3%, giving confidence in the calibration.

Instrument and response lamp stability were primarily assessed using three parameters:

- Measurements of the Total Scene Irradiance (TSI) sensor during response lamp scans
- Photomultiplier Tube (PMT) current at several wavelengths during response lamp scans
- Ratio of TSI signal during solar measurements and weighted solar spectral measurements, where the weighting function is the TSI responsivity. This ratio is denoted "TSI-ratio" in the following.

Note that the TSI sensor is completely independent from possible monochromator and PMT drifts, whereas the PMT current is affected by all system parts, including response lamp, monochromator and PMT, and is also sensitive to temperature changes and high voltage applied. PMT current therefore also provides valuable insight into possible drifts of these components. The only components that the spectroradiometer and TSI have in common are the entrance optics. The TSI ratio is therefore a very sensitive tool to investigate the stability of monochromator, PMT, and electronics.

Figure 5.5.11 shows the PMT current at 300 and 400 nm and the TSI behavior during the whole 1997/98 Ushuaia season. All data is normalized to the averages of the individual system parameters of the whole period. As can be seen from the plot, there are a lot of missing response scans in Period 3. The PMT currents and TSI readings of the "good" scans, however, are stable to within ±4%. During Periods 1 and 2

the stability is even on the ±1.5% level. Beginning in Period 3, the response lamp appears to drift with time. It is possible that the lamp was operated at too high a current in Period 3 as a result of the wobbly terminal contact. This might have triggered the enhanced aging in Periods 4 and 5.

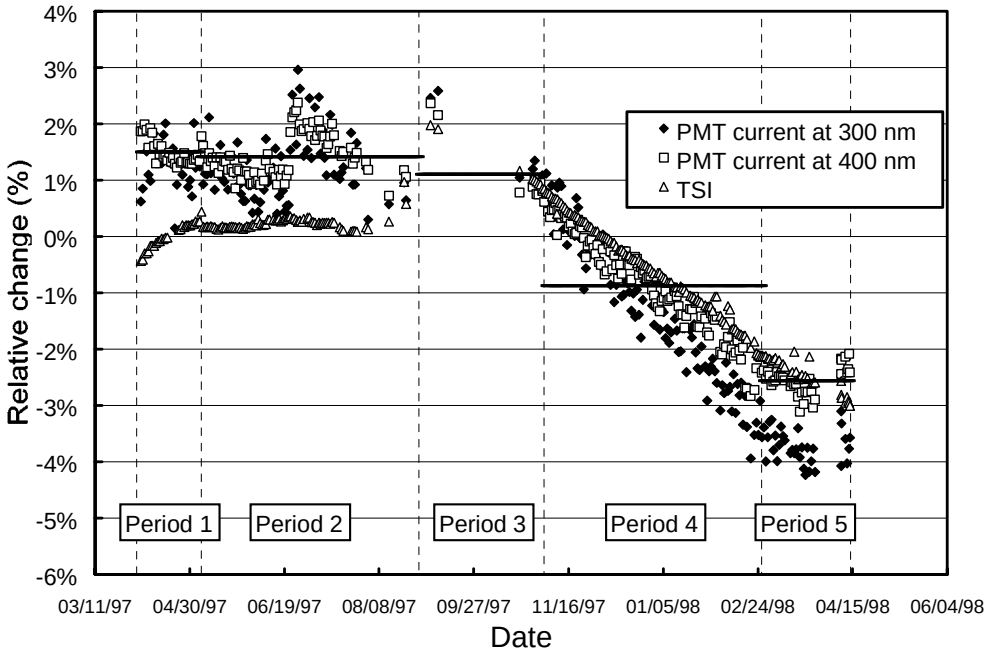

Figure 5.5.11. *Time-series of PMT current at 300 and 400 nm and TSI signal during measurements of the response lamp in the whole Ushuaia 1997/98 season. The data is normalized to the average of the whole season.*

The season is broken into five periods and for each of these periods an average "mean-irradiance" of the response lamp was calculated. Thus the responsivity of the instrument is described by a step function rather than by a smooth variation. This approach has been chosen for practical reasons and has been applied to all sites. The magnitude of these steps is indicated in Figure 5.5.11. The black lines show for each period the average PMT current at 400 nm when measuring the response lamp. The maximum step height is 2%. Because of the step in the responsivity files, solar measurements on the last day of Period 3 will be about 2% lower than measurements on the first day of Period 4. Since TSI measurements accompanying solar scans are not affected by changing responsivity files, a 2% step is also visible in the TSI-ratio, as shown in Figure 5.5.17.

Figure 5.5.12 through Figure 5.5.16 show the behavior of PMT currents and TSI output during response scans separately for each period. The data has been ratioed against the average of all measurements in the given period.

Figure 5.5.17 shows the ratio of TSI measurement and solar irradiance weighted with the TSI responsivity. Only measurements with an SZA between 70° and 80° were used and all values are normalized to the average ratio. Most ratios lie in a band and fewer ratios are above this band. The upper limit of this band varies between 1.06 in Period 3 and 0.99 in the middle of Period 2, with the lowest ratio on 6/21/97, the day of solstice (low ratio at solstice was also observed at other sites). The plot indicates that the spectroradiometer was stable to within ±2% in Period 3, which is the time interval most affected by missing response scans. Note that the TSI-ratio is a more indirect way to track the stability of the instrument than monitoring response lamp scans. Not all structures in the ratio are instrument related but are rather caused by the atmosphere's influence. For example, if the actual response function of the TSI deviated from the weighting function used to convolute the spectral measurements, the ratio will become sensitive on SZA, ozone, and other atmospheric parameters. A slightly different angular response of TSI and

spectroradiometer, as well as time-shifts may also contribute to the observed structures in the ratio. There is some indication that the ratios lying above the band in Figure 5.5.17, which holds the majority of data points, are linked to conditions when the Sun is not obstructed by clouds.

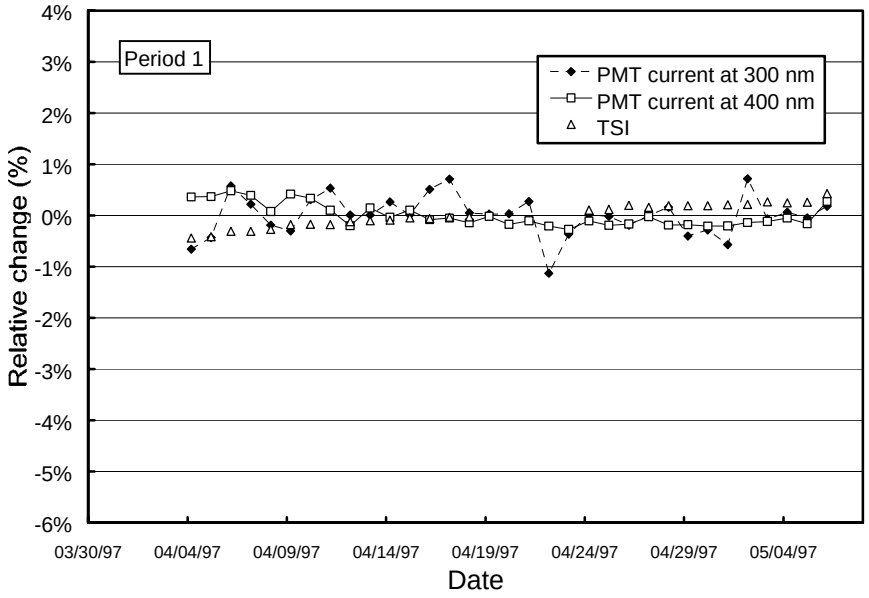

Figure 5.5.12. *Period 1 (4/2/97-5/6/97): All parameters are stable to within ±1%. No response scans are missing.*

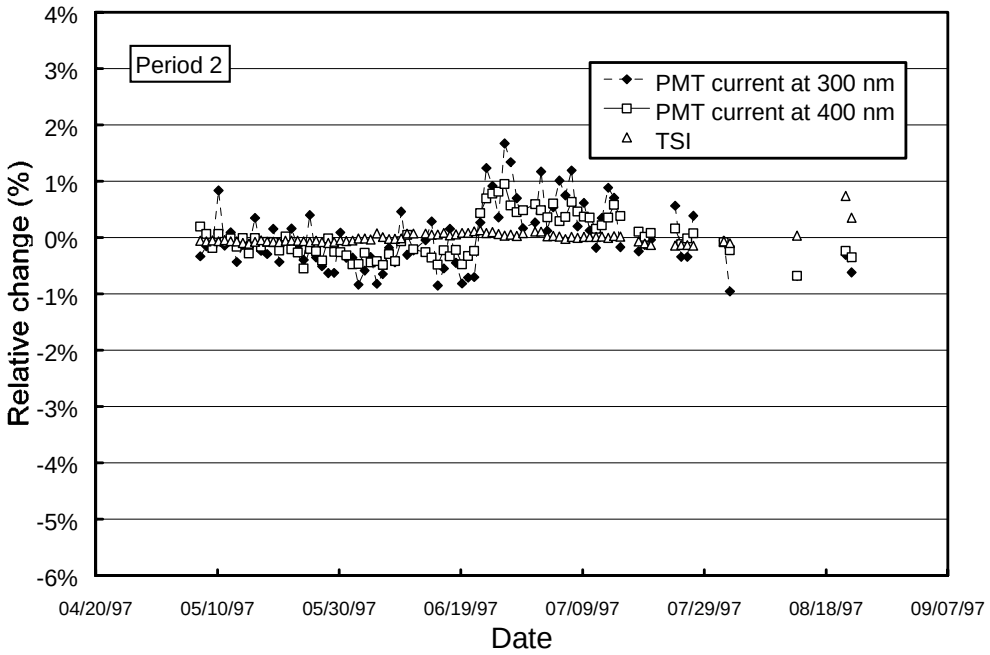

Figure 5.5.13. *Period 2 (5/7/97-8/29/97): The TSI signal is very stable. The PMT currents exhibit a change of approximately 1.5% on day 6/22/97. This is a strong indication that the responsivity, rather than the response lamp, has changed around this day. At the end of the system period some response scans are missing*

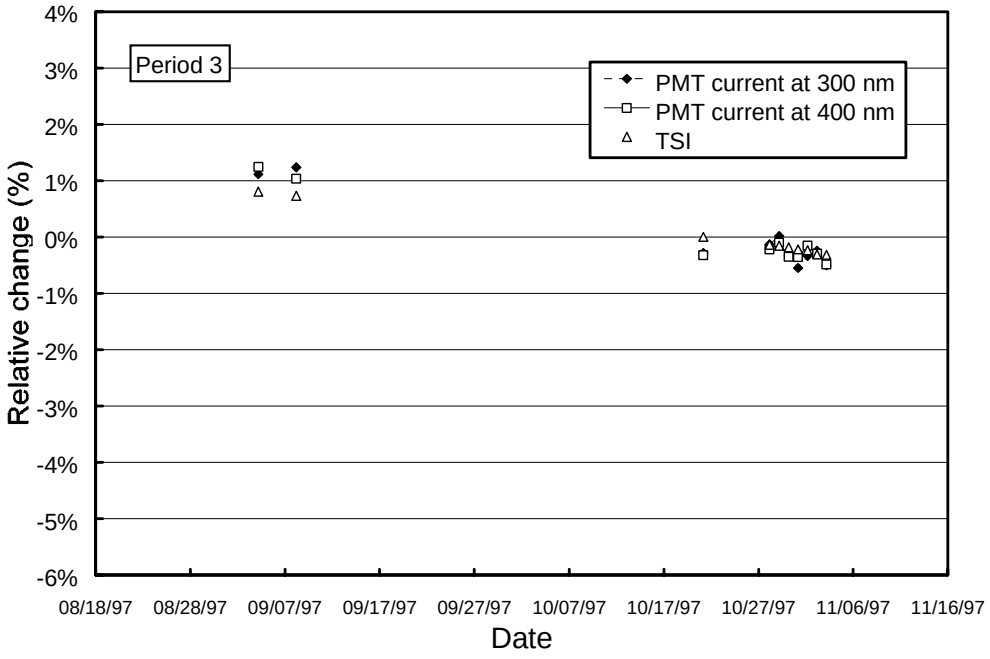

Figure 5.5.14. *Period 3 (8/30/97-11/3/97): The period includes only a few usable response scans.*

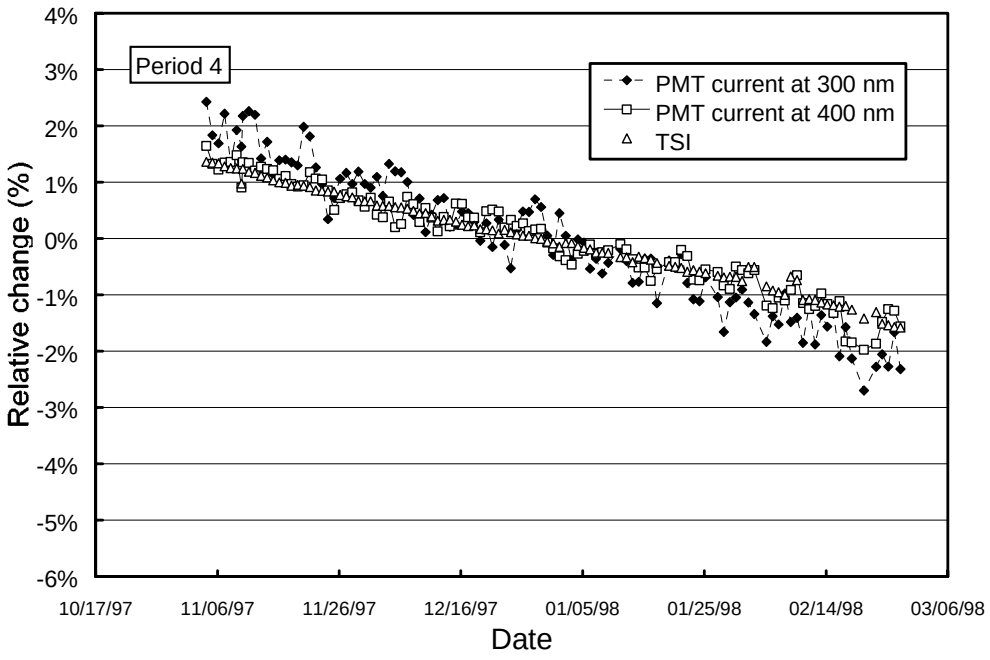

Figure 5.5.15. *Period 4 (11/4/97-2/26/98): All parameters show a downward trend of 2.5%. The instrument itself was stable, since the TSI and PMT current change are in agreement.*

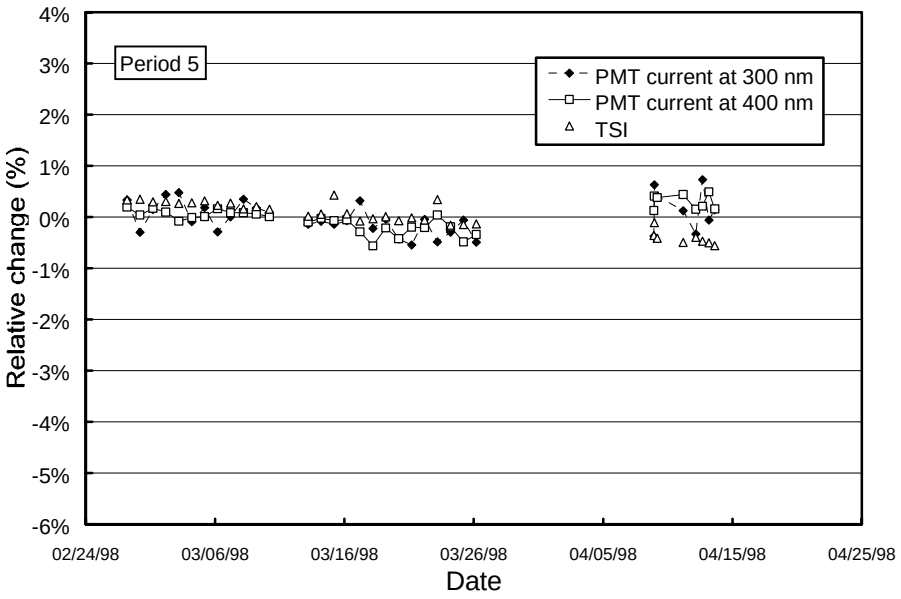

Figure 5.5.16. *Period 5 (2/27/97-4/14/97): All parameters are stable to within ±0.5%. During the gap between 3/27/98 and 4/8/98 the roofbox of the instrument was sealed and no measurements were taken.*

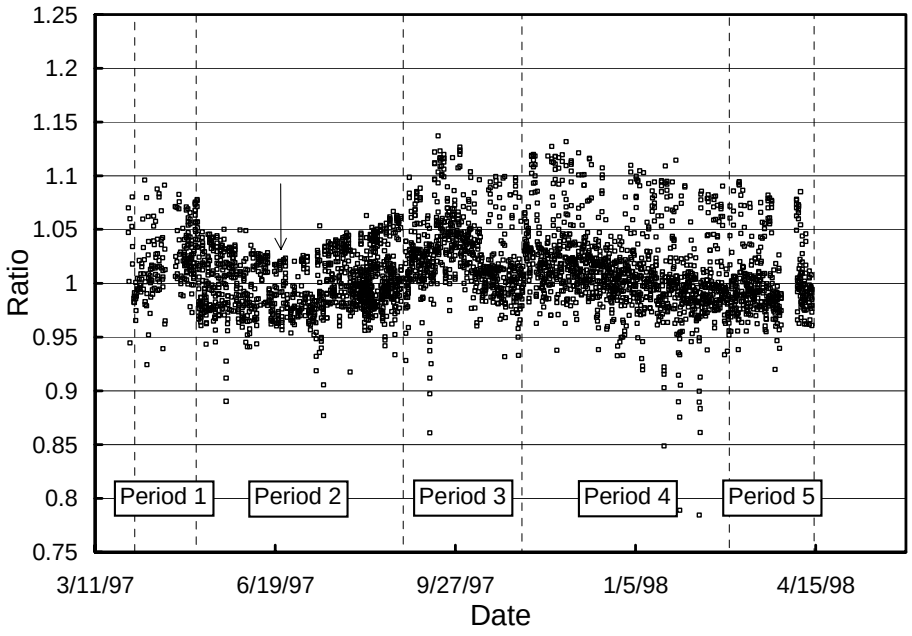

Figure 5.5.17. *Ratio of TSI signal and spectral measurements that were weighted with the spectral responsivity of the TSI. Only measurements with an SZA between 70° and 80° were used. Most ratios lie in a band, the upper limit of which varies between 0.99 in the middle of Period 2 and 1.06 in Period 3. The minimum on day 6/21/97 appears at the solstice. The plot indicates that the spectroradiometer was stable to within ±2% in Period 3, which is the time interval most affected by missing response scans.*

For each of the five periods, a mean irradiance of the response lamp was calculated. From each of the 200-Watt calibrations that took place in a given period, an irradiance spectrum of the response lamp was calculated and the mean irradiance was derived by averaging over these spectra. (For more details about the definition of the "mean irradiance," see Section 3). In addition to the average, the standard deviation was derived from the individual calibration response lamp spectra. Figure 5.5.18 shows the ratios standard deviations / average for all five periods. Thus the plot gives some information on the variability of the calibrations carried out in a specific period. Except for Period 1, the standard deviation in the visible is about 1 to 1.5% of the average and increases to about 2.5% in the short-wave UV-B. The curves for these periods resemble each other very well. For Period 1, however, the standard deviation is significantly increased and reaches values of about to 3 to 3.5% in the UV-B. The response lamp's mean-irradiance in the short Period 1 is based on 3 calibrations only, which are not as consistent as for the other periods. This explains the higher standard deviation.

Figure 5.5.19 compares the mean-irradiances that have been applied to the response lamp in all periods. The functions are plotted against their average. Note that these functions do not represent the true change of the response lamp's irradiance over time, which is a smooth function as indicated in Figure 5.5.11. In contrast, the five discrete functions represent the irradiances, which have been *assigned* to the lamp, in order to facilitate processing of the data. The functions for Periods 2 and 3 are almost identical; at 400 nm, the function for Period 4 is about 2% lower. This is consistent with Figure 5.5.11 Here the solid black line, which represents average PMT current at 400 nm also changes by 2% between Periods 3 and 4. Similarly, the difference of the mean-irradiances for Periods 4 and 5, as shown in Figure 5.5.19, is about 1.1% and this is in agreement with the change of the average PMT current at 400 nm depicted in Figure 5.5.11. The difference between the functions for Periods 1 and 2, however, is not consistent with the change of the instrument parameters. The average of the PMT current in Periods 1 and 2 is about the same (Figure 5.5.11.) whereas the calculated mean irradiances differ by 2.5%. As already mentioned above, the irradiance for Period 1 is based on only three calibrations, which show a higher-than-normal scatter. We conclude that the calibration for this period is problematic; the solar irradiances calculated for this period may be low by 2 to 3%. Also the TSI ratio shows a 3% jump between Periods 1 and 2 in Figure 5.5.17.

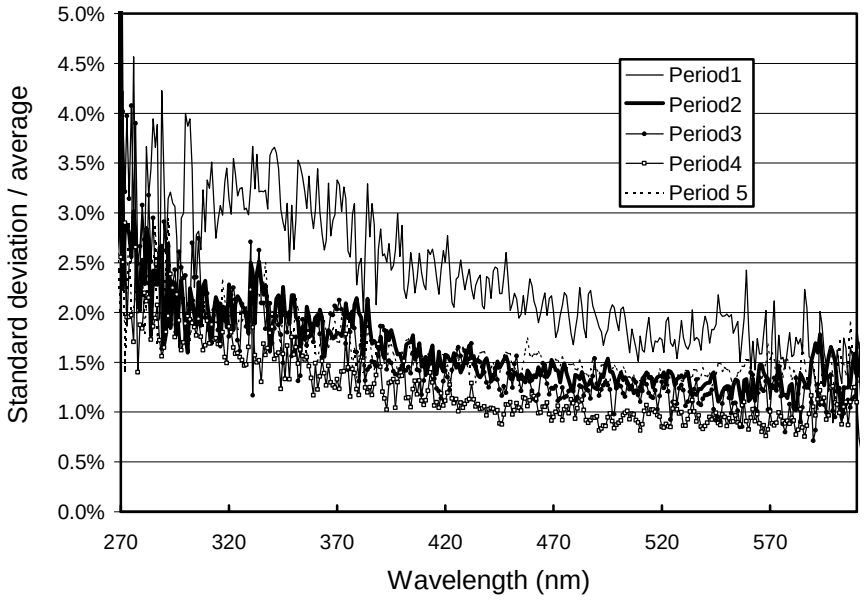

Figure 5.5.18. *Ratio of standard deviation and average calculated from the absolute calibration scans in Period 1- 5 for Ushuaia.*

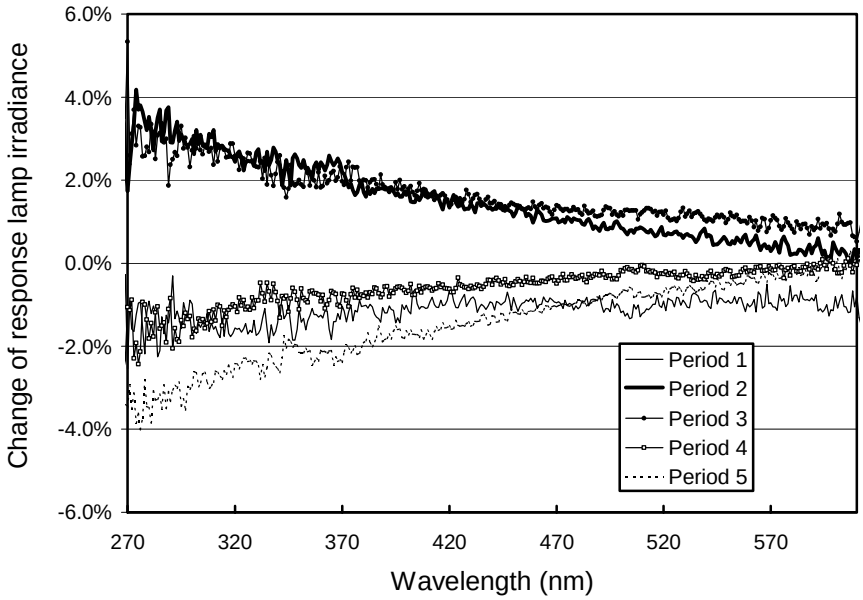

Figure 5.5.19. *Ratios of the response lamp's mean irradiance assigned in each period against the average of all periods.*

5.5.3.3. Lamp Intercomparison

The site standards for the Volume 7 Ushuaia season were the lamps M-698, M-766, and 200W008. M-766 had been the site standard in previous seasons, and had a calibration by Optronic Laboratories of October 1992. For it use hours, this lamp's calibration was dated, therefore the lamp was recalibrated during the 1998 site visit using the BSI traveling standard M-874 (See Section 3 for details on BSI calibration of 200-Watt lamps). Twice Optronic Laboratories calibrated M-874; in 1995 and again in 1998 - approximately half a year after the Ushuaia sites visit. The irradiance table of the 1998 calibration was used for the recalibration of M-766.

Lamp M-698 is a site standard calibrated on-site by intercomparison with lamp M-874, also during the 1998 site visit. Lamp 200W008, also a site standard, was calibrated by Optronic Laboratories in 1996, used for the Ushuaia Volume 7 season.

Figure 5.5.20 shows a comparison of all lamps based on measurements carried out on day 4/11/98 when the lamps were operated one after another. All lamps were compared to M-766. As can be seen, lamps M-698, M-766, and M-874 agree to within ±1%. This is to be expected because of the calibration of M-768 and M-766 with M-874. Compared to this cluster, the calibration of 200W008 is lower by about 2%. One explanation for this deviation is that the Optronic Laboratories irradiance scale has changed by 2% between 1995 and 1998, as discussed in Section 3.3.2.4. If the Optronic Laboratories calibration values of M-874 from 1995, rather than from 1998, had been used, the difference between M-874 and 200W008 (calibrated in 1996) would almost disappear. However, we decided to use the values from 1998 because they are more recent.

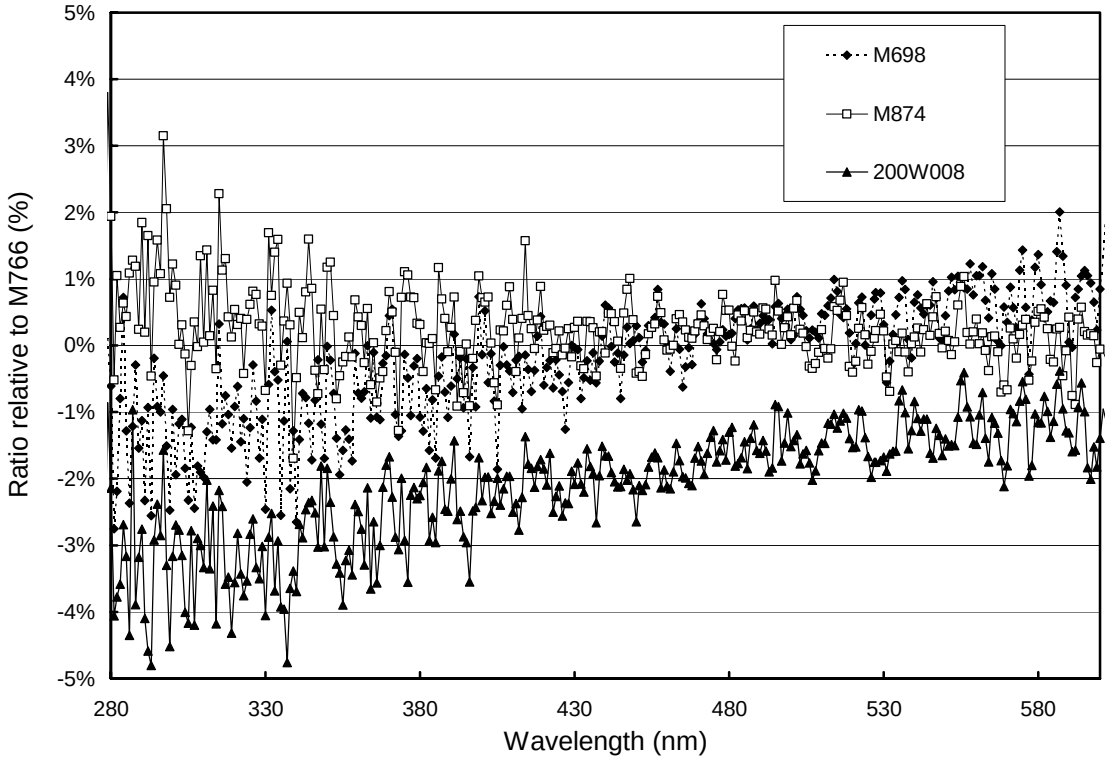

Figure 5.5.20. *Comparison of Ushuaia lamps M-698, 200W008, and the BSI traveling standard M-874 with M-766. All measurements were performed on day 4/11/98 during the season-ending site visit.*

The season-start calibrations on day 3/30/97 appear to be faulty and misleading. For two out of four scans the systems was saturated. Measurements with the third lamp also appear to be defective, therefore no results are presented here. In order to demonstrate that the site standards did not change during the season, Figure 5.5.21 shows a comparison of lamps M-698, 200W008, and M-766 carried out on 7/2/97, about 3 months after the season start. The deviation between the three lamps is the same as in Figure 5.5.17, indicating the stability of the lamps. M-874 is not included in the plot because it is the traveling standard and was therefore not available mid-season.

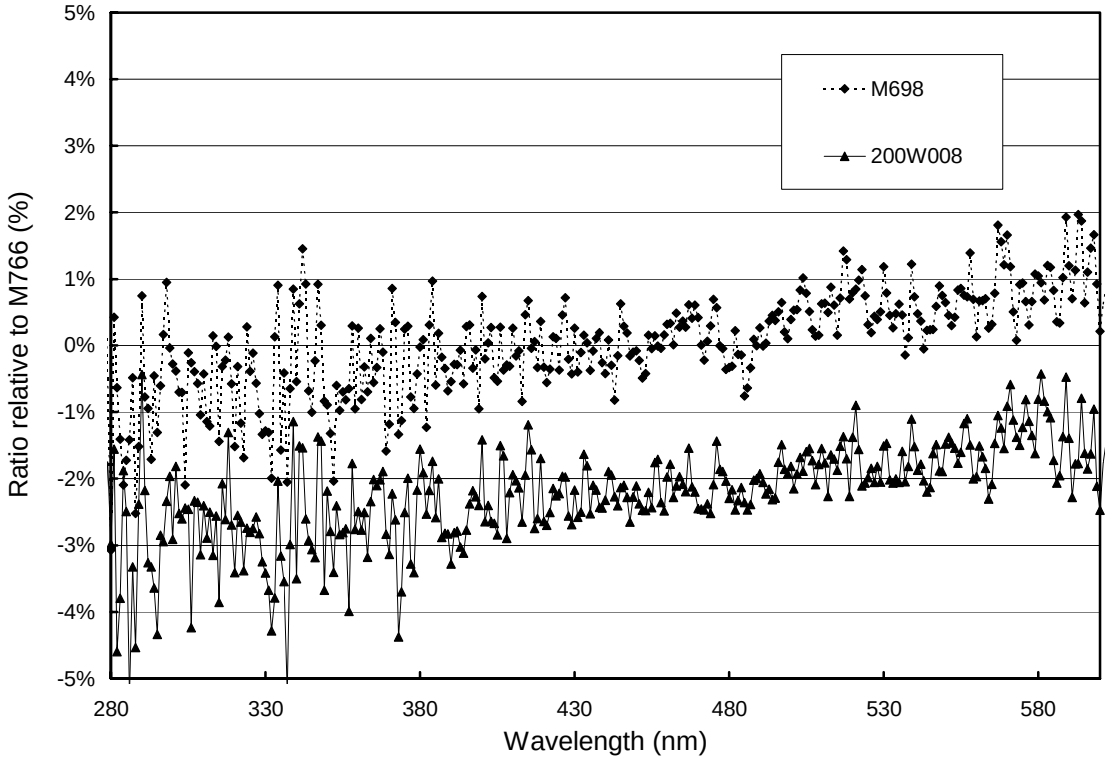

Figure 5.5.21. *Comparison of Ushuaia lamps M-698, 200W008, with M-766 on day 7/2/97.*

5.5.3.4. Missing Data

A total of 16775 scans with SZA smaller than 92° were scheduled to be measured in the Ushuaia Volume 7 season. This is a substantial increase compared to previous seasons. This enhancement is the result of a change in the scan schedule on day 8/5/97, from 2 scans per hour to 4 scans per hour. 15993 scans, which are 95.3% of the scans scheduled, were actually measured, and 15545 scans (92.7%) are included in Volume 7. The discrepancy of 782 scans between scheduled and measured data scans has several reasons:

- Roughly 140 scans were superseded by absolute scans.
- 388 scans are missing between 3/26/98 and 4/3/98 because of repair of the facility roof. During this time no measurements were performed
- Frequent power outages. For example there are no scans on day 8/15/97 (loss of 40 scans).
- For unknown reasons, the scan schedule was set to hourly scans between 4/24/97 and 4/28/97; 45 scans were lost.

Not all scans measured are included in Volume 7. Some scans were found to be defective and were therefore excluded from the final data set.

- As mentioned earlier, many data scans at the start of the season were measured with a PMT high voltage that was too high, causing saturation. Roughly 250 scans between 4/2/97 and 5/6/97 are affected and these have not been included in Volume 7. Fortunately most of these were scans with a large SZA.

- Twelve scans on days 6/11/97 and 6/12/97 were defective.

- For all 16 scans on day 6/26/97 a correct wavelength calibration could not be established .

- All 87 scans from days 8/28/97 and 8/29/97 had to be excluded. These scans were measured during the period of missing response scans. Since the system itself proved to be stable, data scans in this period were usually paired with good response lamp scans that were measured on days preceding and succeeding the day affected. This procedure could not be implemented for days 8/28/97 and 8/29/97, however, because scans on these days were measured with a different PMT high voltage setting than possible response scan candidates.

- Thirty six scans are missing on 11/9/97 because of problems in the wavelength calibration.